Advances in Engineering Software 102 (2016) 97–104

Contents lists available at ScienceDirect

Advances in Engineering Software

journal homepage: www.elsevier.com/locate/advengsoft

Research paper

Structural design optimization of roof slab of a pool type sodium cooled fast reactor

V Prabhu Raja [a], M Ramu [b,*], P R Thyla [a], Sriramachandra Aithal [c], V Rajan Babu [d], P Chellapandi [e]

[a] Department of Mechanical Engineering, PSG College of Technology., Coimbatore, India.
[b] Department of Mechanical Engineering, Amrita School of Engineering, Coimbatore, Amrita Vishwa Vidyapeetham, Amrita University, India.
[c] Reactor Design Group, Indira Gandhi Centre for Atomic Research, Kalpakkam, India
[d] Director (T), Bharatiya Nabhikiya Vidyut Nigam Limited, Kalpakkam, India
[e] Ex-CMD, Bharatiya Nabhikiya Vidyut Nigam Limited, Kalpakkam, India

ARTICLE INFO

Article history:
Received 16 June 2016
Revised 30 August 2016
Accepted 25 September 2016

Keywords:
Roof slab
Optimization
Structural integrity
Numerical analysis

ABSTRACT

The roof slab of the nuclear reactor supports all the components of the reactor. Roof slab is essentially a box structure with top and bottom plates interconnected by vertical shells and radial stiffeners welded to them. The gap between the top and bottom plates is filled with concrete that provides biological and thermal shielding in the top axial direction of the reactor. The 500 MWe Prototype Fast Breeder Reactor (PFBR) is designed based on the Operating Basis Earthquake (OBE) and Safe Shutdown Earthquake (SSE) which are categorized under level A and level D loadings respectively. The primary objective of this work is to optimize the design of the roof slab and to predict and ascertain the structural integrity of the optimized roof slab under static, harmonic and seismic loading conditions. Regression models for critical design parameters are developed and are used in the optimization algorithm.

1. Introduction

Fast Breeder Reactor (FBR) is a sodium cooled pool type reactor with two primary pumps and two secondary loops. A few significant structural dynamics problems such as pump induced as well as flow induced vibration and seismic excitation is very critical in a fast breeder reactor. Roof slab, which is the top cover for the main vessel forms the top shield along with rotating plugs. It provides biological and thermal shielding in the top axial direction of the reactor. It also acts as a support for various components such as main vessel (MV), Intermediate Heat Exchangers (IHX), Decay Heat Exchangers (DHX), Control Plug (CP), Primary Sodium Pump (PSP), in-vessel transfer machine, etc.

The reactor assembly of prototype fast breeder reactor is shown in Fig. 1 and roof slab is shown in Fig. 2. Chetal et al [1] described the salient features of PFBR including the design of the reactor core, reactor assembly, main heat transport systems, component handling, steam water system, electrical power systems, instrumentation and control, plant layout, safety, research and development. Commercial Fast Breeder Reactors (CFBRs) are planned to be built by 2023 after PFBR [2]. CFBR have many innovative features in reactor assembly design to achieve cost reduction. The design adequacy of PFBR components has been confirmed jointly by the scientists of IGCAR and other researchers from academia using several analyses. Chellapandi et al [3] predicted the vibration response of primary pump as well as dynamic forces developed at its supports using numerical analysis. Chellapandi et al [4] have investigated the effect of inter-connection of the nuclear reactor with the adjacent building during seismic event.

Chellapandi et al [5] have investigated the seismic analysis of reactor assembly considering the fluid-structure interaction effects. An axisymmetric finite element analysis is performed with Fourier option to account for the circumferential load variations. The reactor assembly components were modeled as axisymmetric shell structures with FEM. Prakash et al [6] discussed on the experiments carried out of PFBR subassemblies for its design qualifications. The tests include pressure drop measurements, cavitation testing, flow induced vibration studies and subassembly hydraulic lifting studies.

Prakash et al [7] performed the flow induced vibration studies on a scaled down model of PFBR control plug. From the experimental results, it is concluded that the control plug internals are subjected to flow induced vibration away from the resonance and the level of vibration and the bending stress induced are well

* Corresponding author.
E-mail address: m_ramu@cb.amrita.edu (M. Ramu).

http://dx.doi.org/10.1016/j.advengsoft.2016.09.006
0965-9978/

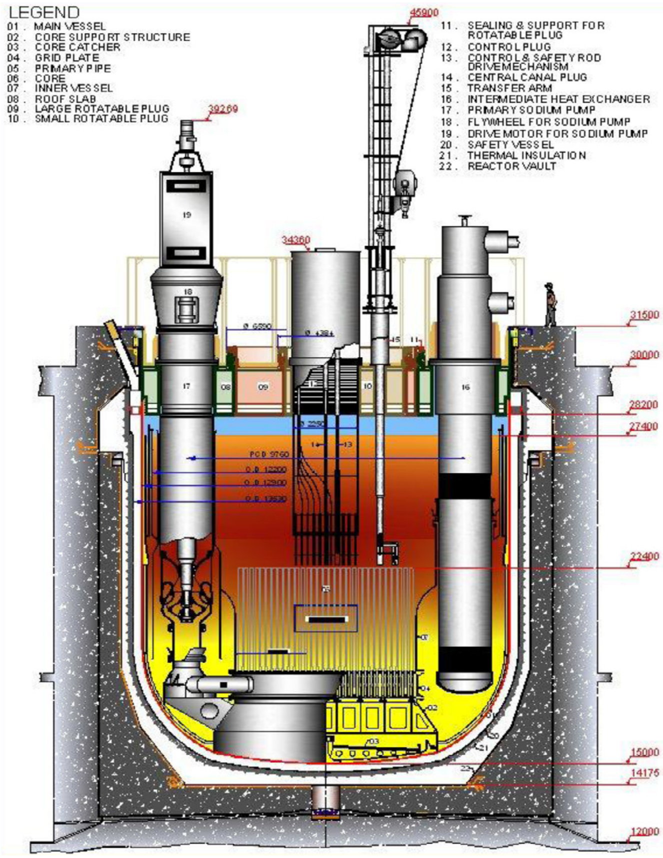

Fig. 1. Schematic of PFBR reactor assembly.

Fig. 2. Typical view of roof slab (top plate removed for clarity).

below the permissible limit. Chellapandi et al [8] have investigated the issues related to structural integrity of primary containment and reactor containment building of PFBR under core disruptive accident condition. Prabhu Raja et al [9] have carried out an investigation of the roof slab based on 1/12th scaled down model made of perspex material.

Constructional experiences show that FBR is costly by a factor of 2 or 3 than pressurized water reactors. Therefore considerable cost reductions are required for their commercialization. Cost of FBR involves construction cost, operation and maintenance cost and fuel cost, of which construction cost alone accounts for 75% of the total cost. The objective of the present study is to minimize the cost of the roof slab by varying the thicknesses of the various plates of roof slab and the height of the roof slab. In this present study, an attempt was made to optimize the existing roof slab design and the optimized roof slab was checked for the design adequacy using harmonic and seismic analysis.

2. Finite element modeling

A parametric model of the roof slab developed using the finite element analysis package ANSYS is shown in Fig. 3. The finite element meshing of the model is done with SHELL63 elements. The SHELL63 element has both bending and membrane capabilities and in-plane and normal loads are permitted [10]. The element has six degrees of freedom at each node: translations in the nodal x, y, and z directions and rotations about the nodal x, y, and z axes. In order to ensure that a mesh independent solution is obtained, seven finite element models were examined with different number of elements. It is found that the difference in results obtained using fourth and fifth models in terms of stress intensity is 0.03% which is very less and hence the fourth model is adopted for further numerical simulation.

Fig. 4 shows the finite element model of the roof slab. The loads of the components supported over the roof slab can be incorporated in the model using two methods: (i) uniformly distributed pressure load and (ii) load per node. In the first method, the weights of the components are converted as uniformly distributed pressure loads by dividing the component weight with the respective surface area over which the component is seated. In the second method, the component weights are converted into load per node, i.e., by dividing the component weight with the total number of nodes attached to the respective surface area over which the component is seated.

In the current analysis, the weights of various components supported by the roof slab are incorporated as weight per unit area on the supporting flanges. An additional flask load of 250 t is considered at PSP/IHX location (one location at a time). The concrete is filled within cooling box sectors and the concrete load acts on the bottom plate through the contact edges of the cooling box sectors (Fig. 5). The weight of the shielding concrete is applied as load per unit node on the nodes of the bottom plate interconnected to contact edges of cooling box sectors.

The incorporation of loads acting on the roof slab has been verified with the reaction forces obtained using the finite element model.

3. Optimization of the roof slab

The objective of the optimization is to reduce the weight of the roof slab within the limit of state variables. Optimization is carried out by two methods: (i) using ANSYS optimization module and (ii) Meta model based optimization. The former method employs a parametric model of the roof slab for optimization within the limitation of state variables. In the later method, a metamodel of the roof slab was developed using Response surface methodology (RSM). Metamodels are a cheaper alternative to costly analysis tools such as finite element method and can significantly reduce the computational time involved.

RSM involves the use of design of experiments for proper sampling of the design space and metamodeling techniques for the development of metamodel. The experimental design adopted for the study was Central Composite Design (CCD) and Orthogonal Array (OA). The metamodeling technique used in this study is polyno-

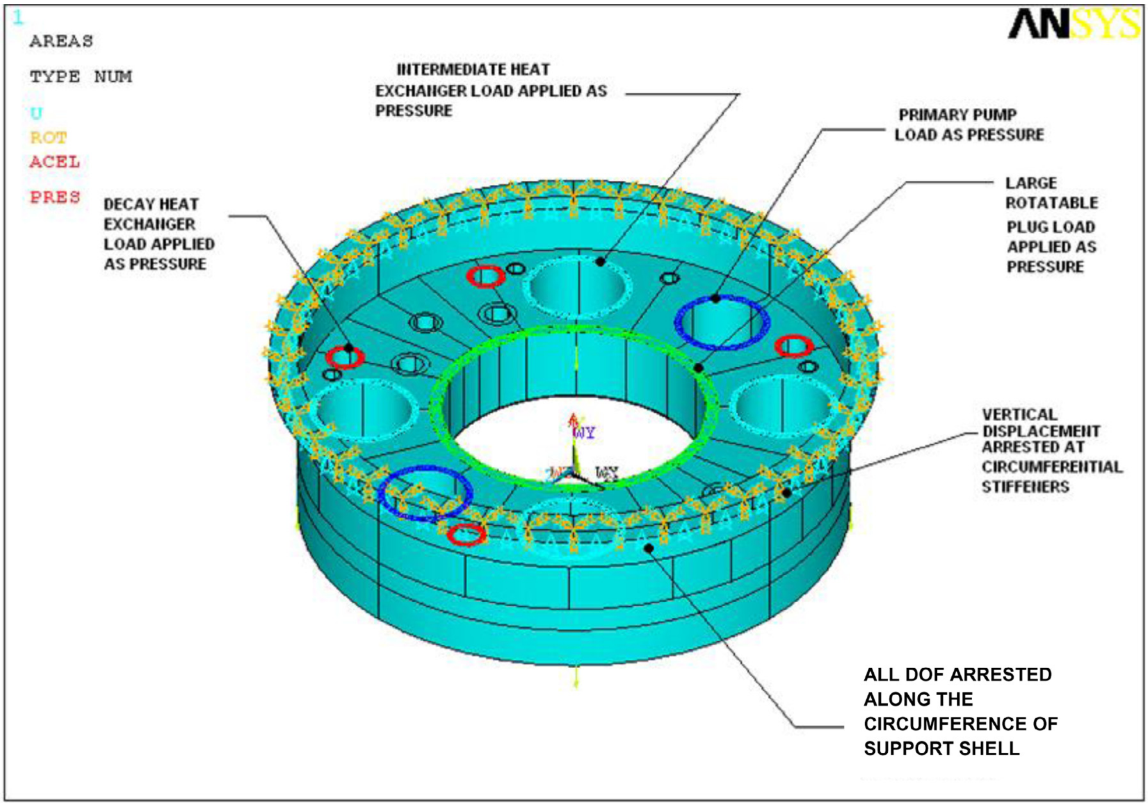

Fig. 3. Parametric model of the roof slab with applied boundary conditions.

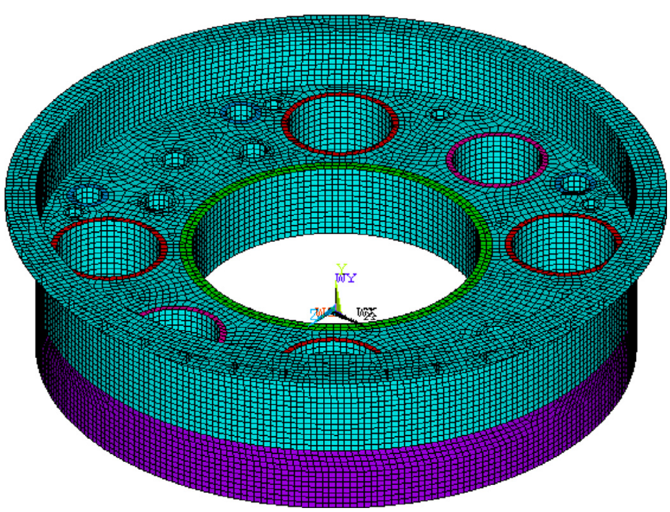

Fig. 4. Finite element model of the roof slab.

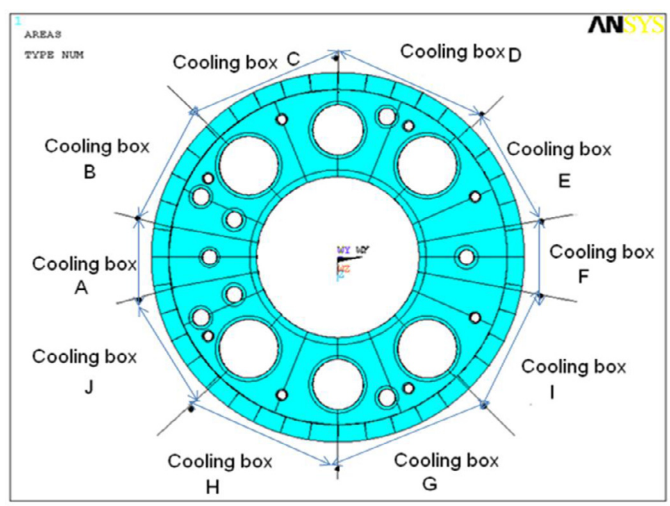

Fig. 5. Roof slab model showing the cooling box sectors.

mial regression and has been applied by a number of researchers [11–15] in designing complex engineering systems.

The design variables considered for the analysis (Fig. 6) are Height of the roof slab (H), Top and Bottom plate thickness (T_1), Inner shell thickness (T_2), Outer shell thickness (T_3), Stiffener thickness (T_4) and IHX, PSP shell thickness (T_5). Sensitivity analysis is performed to determine the effect of variation of independent variables on the dependent functions, viz., deformation and stress in the roof slab. The independent variables are varied within respective ranges and their effect on the objective and constraint functions are noted.

The sensitivity analysis reveals that deformation and stress are relatively less sensitive to the parameters 'T_2' and 'T_5' as shown in Figs. 7 and 8 and therefore the above two parameters have not been considered for the optimization process.

The most widely used response surface approximating functions are low-order polynomials. For significant curvature, a second order polynomial which includes all two-factor interactions can be used. A second order polynomial model can be expressed as:

$$\hat{y} = \beta_0+\beta_1 x_1+\beta_2 x_2+\ldots+\beta_k x_k+\beta_{12} x_1 x_2+\ldots+\beta_{k-1,k} x_{k-1} x_k + \beta_{11} x_1^2+\beta_{22} x_2^2+\ldots+\beta_{kk} x_k^2 \quad (1)$$

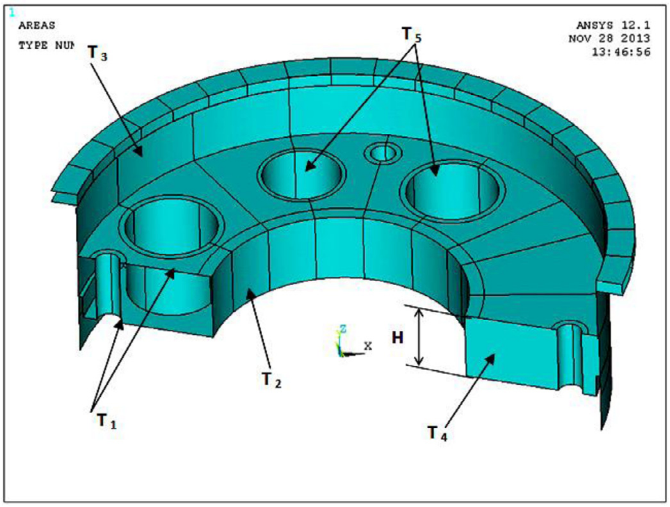

Fig. 6. Parametric dimensioning of the roof slab model.

Table 1
Performance measures of metamodels.

Performance measure	Volume	Stress	Deflection
R^2	0.999	0.895	0.986
Relative error in %	3.05	6.55	6.10

The parameters of the polynomial in Eq. (1) are usually determined by least squares regression analysis by fitting the response surface approximations to existing data. For the roof slab optimization problem, three metamodels are generated to approximate the total volume of roof slab, stress developed and deflection using L32 array computer experimentation. In order to validate the metamodel some random experiments were conducted and compared with the finite element simulation of the actual model. Table 1 shows the fitness of the metamodels. Regression models of the three responses generated are given by the Eqs. (2)–(4)

$$\begin{aligned}\text{Volume} = & -42.48 + 14.92T_1 + 28.74T_3 + 84.87T_4 + 59.61H \\ & - 619.77T_1T_3 + 321.08T_1T_4 + 9.45T_1H - 1392.13T_3T_4 \\ & + 123.22T_3H + 68.55T_4H + 2363.36{T_1}^2 + 2194.4{T_3}^2 \\ & - 2730.59T_4 - 18.87H^2 \end{aligned} \tag{2}$$

$$\begin{aligned}\text{Deflection} = & -4.65 \times 10^{-2} + 0.246T_1 - 1.23 \times 10^{-2}T_3 \\ & + 5.148 \times 10^{-2}T_4 + 0.044H + 0.227T_1T_3 + 1.23T_1T_4 \\ & - 0.102T_1H + 0.357T_3T_4 - 0.275 \times 10^{-2}T_3H \\ & + 0.783 \times 10^{-2}T_4H - 1.12{T_1}^2 + 0.956{T_3}^2 \\ & - 2.164{T_4}^2 - 1.17 \times 10^{-2}H^2 \end{aligned} \tag{3}$$

$$\begin{aligned}\text{Stress} = & 2.39 \times 10^9 - 2.99 \times 10^9H - 10.7 \times 10^9T_1 \\ & + 13.30 \times 10^9T_3 - 6.14 \times 10^9T_4 + 6.05 \times 10^9HT_1 \\ & - 6.63 \times 10^9HT_3 + 2.78 \times 10^9HT_4 + 93.2 \times 10^9T_1T_2 \\ & + 25.4 \times 10^9T_1T_4 + 26.40T_3T_4 + 0.854 \times 10^9H^2 \\ & - 12 \times 10^9{T_1}^2 - 32 \times 10^9{T_3}^2 + 9.15{T_4}^2 \end{aligned} \tag{4}$$

The metamodel developed for volume is more accurate compared to that of stress and deflection with a maximum error of 6.55% for stress. The method of probabilistic search based on evolutionary algorithms is chosen for the present optimization problem. Genetic Algorithm (GA) is a globally optimal method motivated from natural evolutionary concepts. Two different kinds of GA operations, namely, binary coding and real coding GA are available for solving any optimization problem. In general, a real-coded GA is more suitable and convenient to deal with most of the practical engineering applications.

The Real-Coded Genetic Algorithm (RCGA) developed by Deb [16] is used for obtaining the optimum design of roof slab. Certain modifications in the algorithm of this program were necessary to apply the same for the present study. RCGA has been developed for four input variables and two constraints. The RCGA parameters chosen are: crossover probability = 0.8, mutation probability = 0.2, number of generations = 100, and the population size = 60.

It was observed that as the population size increased above 60, there was a reduction in the performance of the algorithm. It was also observed that the higher the value of crossover probability, better was the model performance. Metamodel for volume is defined as the objective function, while stress and deflection are taken as constraint functions. The design limits as per RCC MR for the roof slab are set as the limiting values for the constraint functions. Feasible solutions are found out and shown in Table 2 while Table 3 represents the deflection at the inner radius of the roof slab i.e., at Large Rotatable Plug (LRP) flange location.

It is observed that the solution has converged near the deflection limit of 0.005 m rather than the stress intensity of 225 MPa. Also the deflection values are closer to the limit under the application of flask load which occurs during installation or dismantling of IHX/PSP. But during the operation of reactor, the flask load won't be acting and the deflection value will be away from the design limit. After design optimization, the volume of roof slab has been reduced from 19.91 m^3 to 16.04 m^3 leading to a weight reduction of 30.37 tonnes.

4. Structural integrity assessment of roof slab

4.1. *Static analysis of the roof slab*

FBR has to be designed for Operating Basis Earthquake (OBE) and Safe Shutdown Earthquake (SSE) and should satisfy level A and level D loadings respectively as per RCC-MR. The primary stress intensities under normal plus OBE and normal plus SSE should respect the criteria given in Table 4. In addition to the stress limits, the vertical deflection and slope at the inner edge of the roof slab should be restricted within 5 mm and 43.6 x10^{-4} radians respectively.

The optimized roof slab is first checked for the structural integrity under static loading condition. The vertical deflection at the inner edge of the roof slab is significant and it should be within 5 mm. This limit is to avoid excessive reactivity addition due to the motion of control rods supported on roof slab. The maximum stress should not exceed the allowable value mentioned in the RCC-MR 2007 code. The static structural analysis was carried out using finite element analysis package ANSYS. The deformed shape and the stress contour of the roof slab are shown in Figs. 9 and 10 respectively.

4.2. *Harmonic analysis of the roof slab*

A harmonic analysis is used to determine the response of the structure under a steady-state sinusoidal (harmonic) loading at a given frequency. The source of harmonic excitation is Primary Sodium Pump(PSP) vibration. The roof slab is analyzed for the excitation forces caused by PSP unbalance and the result provides the data for checking the acceptability of vibration levels and resonance condition. The harmonic excitation on the roof slab is due to the PSP which rotates at a nominal speed of 590 rpm (9.83 Hz) which can vary between 15% and 100% of nominal speed. Even though the vibration level of PSP is controlled, the induced forces

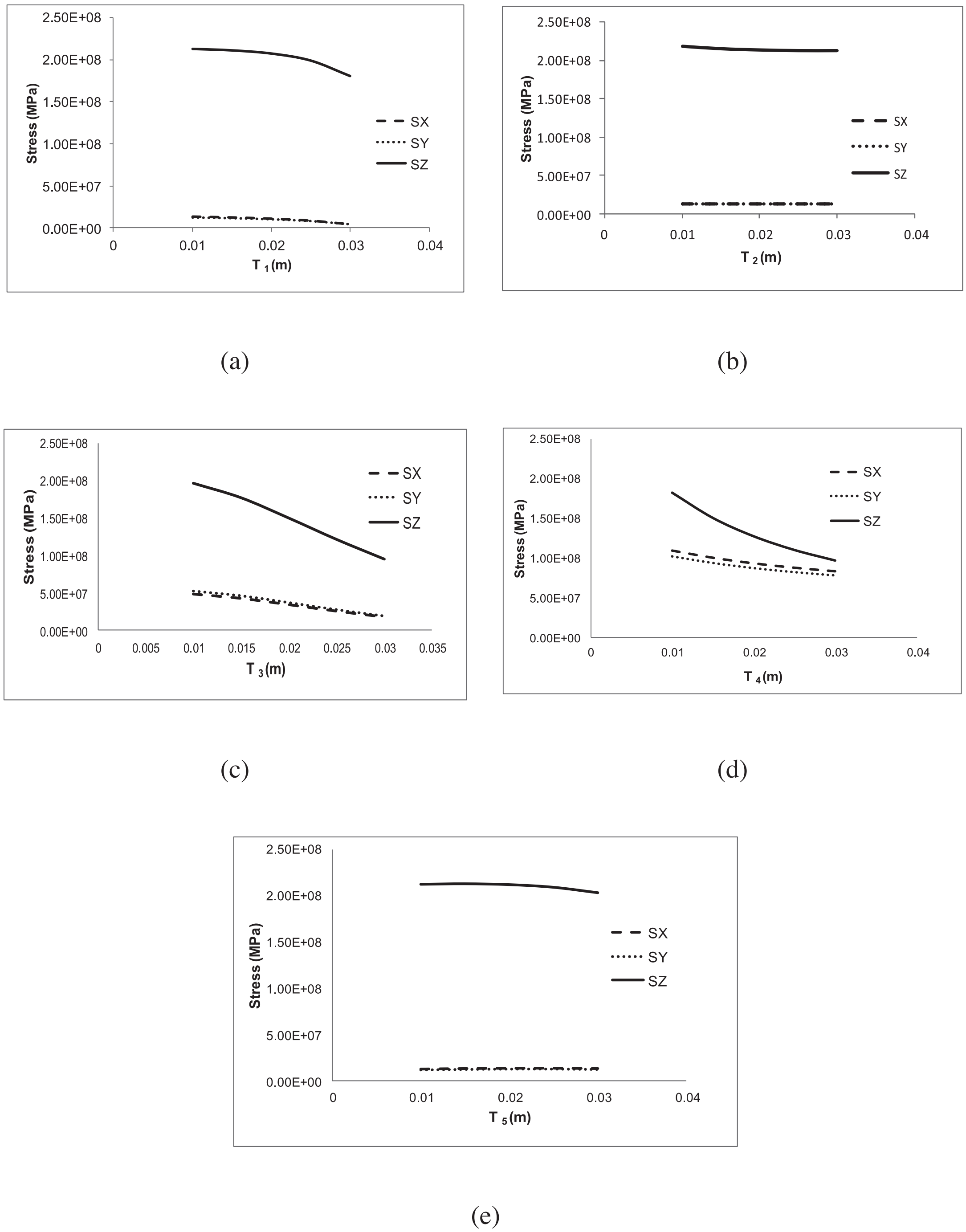

Fig. 7. Influence of various parameters on stress.

Table 2
Optimum design of roof slab.

Details	Design variables in m						Volume (m^3)
	T_1	T_2	T_3	T_4	T_5	H	
Initial design	0.030	0.030	0.030	0.030	0.030	1.800	19.909
Optimum design	0.022	0.015	0.023	0.027	0.015	1.723	14.880
Final design	0.025	0.015	0.025	0.03	0.015	1.725	16.040

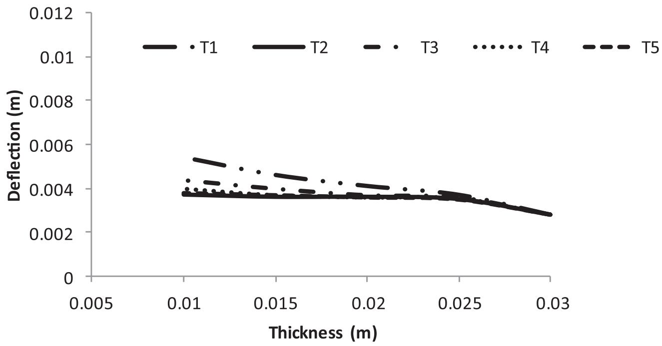

Fig. 8. Influence of various parameters on deflection.

Table 3
Deflection at LRP location for optimum configuration.

Detail	Deflection ($\times 10^{-3}$ m) with flask load
Initial design	3.56
Optimum design	4.94

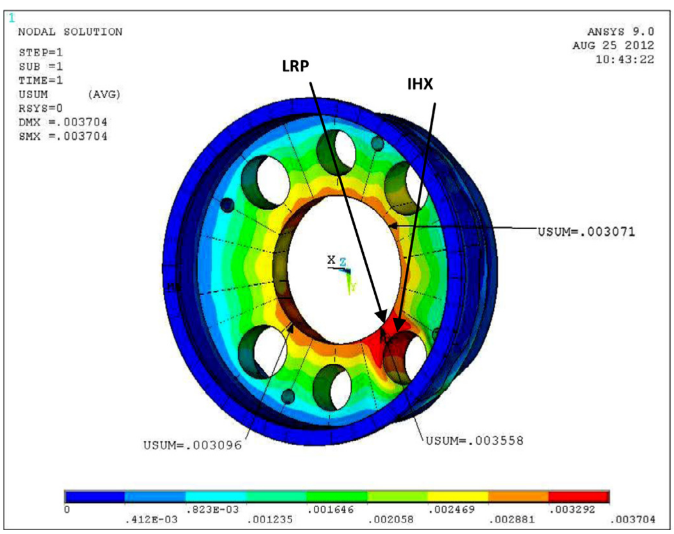

Fig. 9. Deformed shape of the roof slab under static loads.

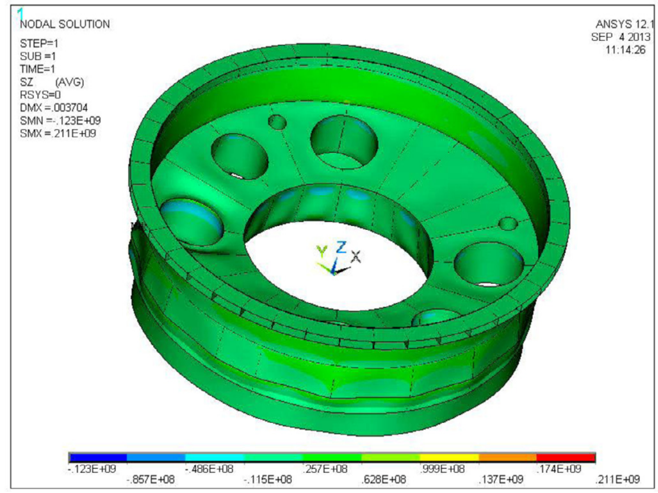

Fig. 10. Stress plot of the roof slab under static loads.

Fig. 11. Finite element model of the roof slab for harmonic analysis.

at the roof slab may cause significant vibration due to resonance. The excitation source is the centrifugal force due to unbalance caused by mechanical misalignment. The product of mass and eccentricity is 4.49 kg m for the unbalanced condition. The unbalance force due to PSP rotor is estimated to be 17.105 kN during the nominal speed. The PSP is not included in the finite element model as such while the operation at the PSP rotor has been modeled as a mass element at its mass center location. The mass center of the rotor is connected to the IHX flanges using rigid links in order to transfer the forces as shown in Fig. 11.

4.3. Seismic analysis of the roof slab

PFBR is designed for two levels of earthquake, called Operating Basis Earthquake (OBE) and Safe Shutdown Earthquake (SSE). Seismic analysis of the roof slab is carried out to ensure that certain functional limits and RCC-MR design criteria mentioned in Table 4 are respected. The important functional requirements that must be addressed during seismic analysis are: (i) the reactivity insertion due to relative vertical displacements between absorber rods and fuel sub-assembly, should not result in super prompt criticality and (ii) there should not be any mechanical interaction between the adjacent shells.

The primary membrane stress intensity (P_m) and the primary membrane combined with bending stress intensities ($P_m + P_b$) are

Table 4
Limits for primary stress intensity.

Stress intensity component, MPa	Static (level A)		Seismic (level D)			
			OBE		SSE	
	Limit	Value	Limit	Value	Limit	Value
Membrane P_m	S_m	150	S_m	150	$2.4 \times S_m$	360
Combined membrane and bending, $P_m + P_b$	$1.5 \times S_m$	225	$1.5 \times S_m$	225	$3.6 \times S_m$	540

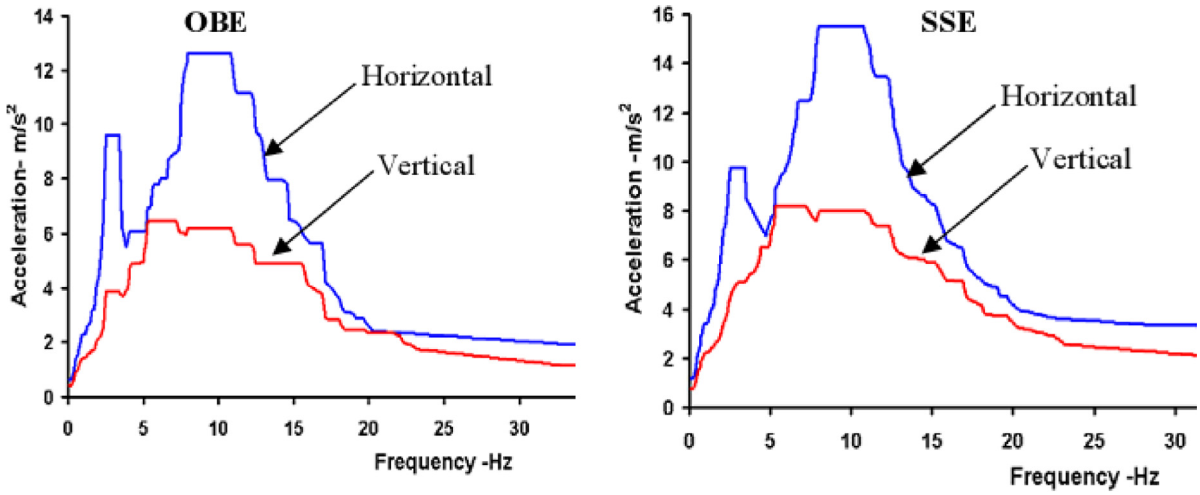

Fig. 12. Floor response spectra at reactor assembly support [4].

extracted and using the stress components, the Major/Minor principal stress corresponding to membrane component are determined using the following relation.

$$\sigma_{1M,2M} = \frac{(\sigma_{XM} + \sigma_{YM}) \pm \left[(\sigma_{XM} - \sigma_{YM})^2 + 4\tau_M^2\right]^{\frac{1}{2}}}{2}$$

Similarly, the major/minor principal stress corresponding to membrane plus bending component are determined using the following relation:

$$\sigma_{1MB,2MB} = \frac{(\sigma_{XMB} + \sigma_{YMB}) \pm \left[(\sigma_{XMB} - \sigma_{YMB})^2 + 4\tau_{MB}^2\right]^{\frac{1}{2}}}{2}$$

Maximum primary stress intensities are computed from the derived results as below:

$P_m = \max\ \{((\sigma_{1M} - \sigma_{2M}),\ \sigma_{1M},\ \sigma_{2M}\}$ where σ_{1M} and σ_{2M} are the major and minor principal membrane stress intensities respectively.

Similarly, $P_m + P_b = \max\ \{((\sigma_{1MB} - \sigma_{2MB}),\ \sigma_{1MB},\ \sigma_{2MB}\}$ where σ_{1MB} and σ_{2MB} are the major and minor principal membrane plus bending stress intensities respectively.

Seismic analysis of the roof slab is carried out on the roof slab using ANSYS software. The seismic excitations at reactor assembly support location at the reactor vault, derived from the results of seismic analysis of entire nuclear island performed by IGCAR, Kalpakkam are employed for the analysis. The basic seismic input data which is site dependent design response spectrum was applied for the 3D seismic analysis of nuclear island including all the essential buildings. Acceleration time histories in two horizontal and vertical directions are extracted at reactor assembly support location are as shown in Fig. 12.

The damping values of 2% for OBE and 4% for SSE which is applicable for the analysis of welded structure as per ASME standards are used.

Table 5
Primary stress intensity based on numerical analysis.

Location	Primary stress intensity (MPa)			Design limit (MPa)
	Static analysis	Seismic-OBE	Seismic-SSE	
1	97.6	74.0	125.9	Static - 225
2	39.7	31.5	45.0	Seismic OBE - 225
3	30.9	28.8	46.1	Seismic SSE - 540
4	17.8	27.9	61.2	
5	34.6	70.9	90.8	
6	25.8	33.8	74.0	
7	38.5	50.8	40.4	
8	44.1	77.7	73.3	
9	30.8	118	108	

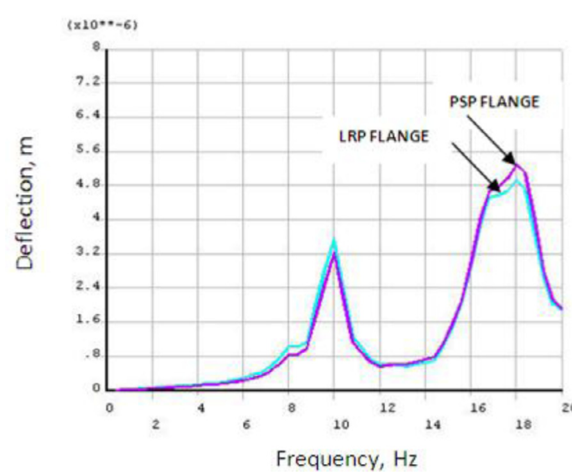

Fig. 13. Dynamic response of the roof slab.

5. Results and discussions

In order to check for the design adequacy of roof slab, the primary stress intensities must be determined as per the procedure mentioned above at critical locations. Nine critical locations in the roof slab have been identified and the membrane and bending resultants are extracted for each element. The primary stress intensity values based on static and seismic analysis are given in Table 5 and are found to be within the design limits. The amplitude of vibration of roof slab under the action of pump induced excitation force is estimated to be 3.6 µm around 10 Hz which matches with the PSP shaft frequency. The dynamic response on the roof slab at the frequency range of 0–20 Hz is shown in Fig. 13.

The amplitude of vibration of the roof response at various frequencies has been retrieved at two locations namely, LRP flange and PSP flange. The dynamic response pattern of the roof slab at nominal operating speed is shown in Fig. 14. The dynamic stresses induced at the different frequencies and at the operating frequency are shown in Fig. 15 and Fig. 16 respectively. Since the order of vibration at other frequencies is insignificant and the induced fluctu-

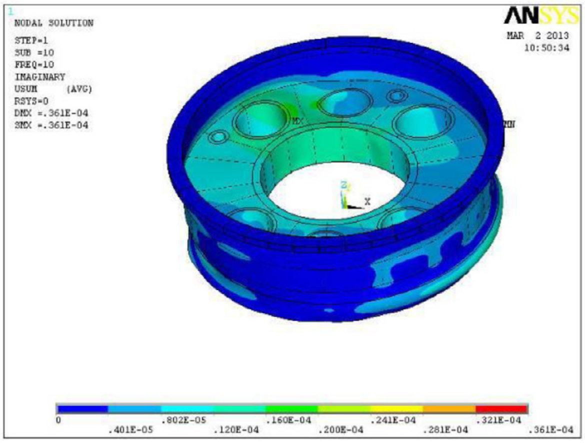

Fig. 14. Typical response of roof slab during PSP operation.

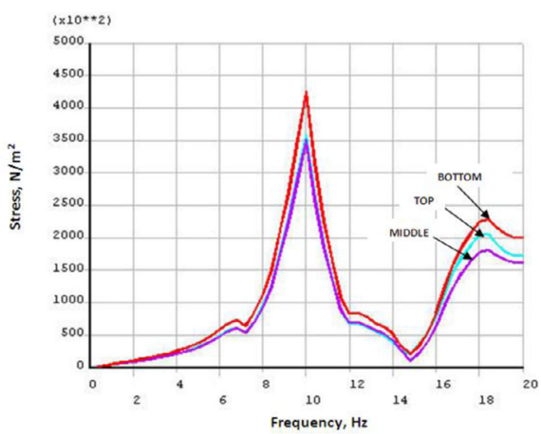

Fig. 15. Dynamic stress induced in roof slab.

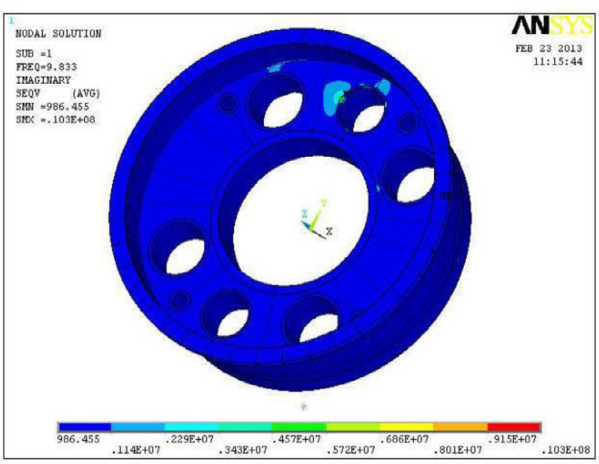

Fig. 16. Dynamic stress in roof slab at the operating frequency.

ating stress is within 3.43 MPa, the design parameters are acceptable.

6. Conclusion

The roof slab considered in this work plays an important role in the structural health of a nuclear reactor as it supports the entire load of the reactor. Hence; the structural integrity assessment of roof slab is mandatory and has been investigated in this work. The prime objective of this work is to carry out design optimization of the roof slab to reduce the overall weight of the nuclear reactor. A metamodel based optimization approach has been adopted in the present work. The design optimization of roof slab using metamodels has yielded a weight reduction of 19.44% as the weight of roof slab is reduced by 30.37 tonnes from the total weight of 155 tonnes. The optimum configuration of roof slab is checked for the design adequacy using static, harmonic and seismic analysis. It is demonstrated based on numerical investigations that the optimized roof slab meets the functional and structural integrity requirements mentioned in the RCC-MR code.

Acknowledgments

The authors are grateful to Mr S C Chetal and Dr Baldev Raj, the then Directors-IGCAR for their continuous encouragement and guidance in carrying out the work. We are indebted to the Management, Principal Dr R Rudramoorthy and the then Head of the Department of Mechanical Engineering-Dr P V Mohanram of PSG College of Technology for providing the necessary facilities to carry out the research work.

References

[1] Chetal SC, Balasubramaniyan P, Chellapandi P, Mohanakrishnan P, Puthiyavinayagam P, Pillai CP, et al. The design of the prototype fast breeder reactor. Nucl Eng Des 2006;236:852–60.
[2] Chellapandi P, Puthiyavinayagam P, Balasubramaniyan S, Ragupathy S, Rajanbabu V, Chetal SC, et al. Design concepts for reactor assembly components of 500 MWe future SFRs. Nucl Eng Des 2010;240:2948–56.
[3] Chellapandi P, Jalaldeen J, Srinivasan R, Chetal SC, Bhoje SB. Vibration analysis of reactor assembly internals for PFBR, Prague, Czech Republic: SMiRT 17; 2003. Paper no. J02_6.
[4] Chellapandi P, Chetal SC, Raj B. Seismic analysis of reactor assembly for prototype fast breeder reactor, Toronto: Transactions, SMiRT 19; 2007. Paper no. K12/3.
[5] Chellapandi P, Chetal SC, Raj B. Effects of nuclear island connected buildings on seismic behaviour of reactor internals in a pool type fast breeder reactor. Nucl Eng Des 2007;237:2250–64.
[6] Prakash V, Thirumalai M, Anandaraj M, Kumar PA, Ramdasu D, Pandey GK, et al. Experimental qualification of subassembly design for Prototype Fast Breeder Reactor. Nucl Eng Des 2011;241:3325–32.
[7] Prakash V, Kumar PA, Anandaraj M, Thirumalai M, Anandbabu C, Rajan KK. Flow induced vibration studies on PFBR control plug components. Nucl Eng Des 2012;250:725–34.
[8] Chellapandi P, Srinivasan GS, Chetal SC. Primary containment capacity of prototype fast breeder reactor against core disruptive accident loadings. Nucl Eng Des 2013;256:178–87.
[9] Prabhu Raja V, Ramu M, Thyla PR, Aithal SR, Rajan Babu V, Chellapandi P, et al. Experimental and numerical investigations on roof slab of a pool type sodium cooled fast reactor based on model studies. Ann Nucl Energy 2015;85:1085–95.
[10] ANSYS Theory Manual, Documentation 9.0.
[11] Engelund WC, Douglas OS, Lepsch RA, McMillian MM, Unal R. Aerodynamic configuration design using response surface methodology analysis, Monterey, CA: AIAA Aircraft Design, System & Operations Management.; 1993. Paper 93-3967.
[12] Unal R, Lepsch RA, Engelund W, Stanley DO. Approximation model building and multidisciplinary design optimization using response surface methods. In: 6th AIAA/USAF/NASA/ISSMO symposium on multidisciplinary analysis and optimization, 1. Bellevue, WA: AIAA; 1996. p. 592–7.
[13] Venter G, Haftka RT, Starnes JH Jr. Construction of response surfaces for design optimization applications. In: 6th AIAA/USAF/NASA/ISSMO symposium on multidisciplinary analysis and optimization, 1. Bellevue, WA: AIAA; 1996. p. 548–64.
[14] Chen W, Allen JK, Mavris D, Mistree F. A concept exploration method for determining robust top-level specifications. Eng Optim 1996;26:137–58.
[15] Simpson TW, Peplinski J, Koch PN, Allen JK. On the use of statistics in design and the implications for deterministic computer experiments. Design theory and methodology - DTM'97, Sacramento, CA: ASME; 1997. Paper No. DETC97/DTM-3881.
[16] Deb K. Multi-objective optimization using evolutionary algorithms. Wiley; 2001.